Egypt. J. Chem. **Vol. 66,** No. 3 pp. 529 - 535 (2023)

Egyptian Journal of Chemistry

http://ejchem.journals.ekb.eg/

Functional Groups, Band Gap Energy, and Morphology Properties of Annealed Silicon Dioxide (SiO_2)

Dyah A.P. Wardani,[a]* Budi Hariyanto,[b] Neny Kurniawati,[b] Nazopatul P. Har,[c] Noviyan Darmawan,[d,e] Irzaman,[c]

[a]*Department of Chemistry, Faculty of Mathematics and Natural Science, Universitas Palangka Raya, Palangka Raya 73111, Indonesia*

[b]*Department of Physics, Faculty of Mathematics and Natural Science, Universitas Palangka Raya, Palangka Raya 73111, Indonesia*

[c]*Department of Physics, Faculty of Mathematics and Natural Sciences, IPB University, Bogor 16680, Indonesia*

[d]*Department of Chemistry, Faculty of Mathematics and Natural Sciences, IPB University, Bogor 16680, Indonesia*

[e]*Halal Science Center LPPM IPB, IPB Unversity, Bogor, 16680, Indonesia*

Abstract

Annealed silicon dioxide (SiO_2) has been prepared by various annealing temperatures at 0 (without treatment, room temperature), 800 °C, 900 °C and 1000 °C denote as S0, S800, S900 and S1000. The properties of the annealed SiO_2 were characterized by three methods. The functional groups were identified using FTIR, the band gap energy was determined using UV-Vis DR, and the morphological properties of SiO_2 were determined using SEM. FTIR data show that the characteristic functional groups of annealed silicon dioxide are Si−O−Si, Si−Si, −OH, H−Si−Si−H (monohydride), dan Si−OH. The band gap energy values for annealed SiO_2 at S0, S800, S900 and S1000 were 2.27; 2.27; 2.26; 2.22 eV. The morphology of silicon dioxide shows that silicon dioxide has irregular shape and size, it has sharp angles accompanied by small flakes on the surface, the particle size is estimated to be around 3-10 μm.

Keywords: annealed silicon dioxide (SiO_2); functional group; band gap energy; morphology.

1. Introduction

Silicon dioxide, SiO_2, is the principal constituent of rock-forming minerals in magmatic and metamorphic rocks. It is also an essential component of sediments and soils [1] . Bound as silicates, it accounts for ca. 75 wt% of the Earth's crust [2]. Free SiO_2 predominantly occurs as quartz, which makes up 12–14 wt% of the lithosphere. SiO_2 crystals are almost pure SiO_2 and do not contain large impurities. Water, however, can be incorporated in concentrations from hundreds to several thousands of parts per million in quartz. The transition from structural incorporation to microstructural inclusion is fluent [3].

Silica also can be produced from plants such as silica from rice husks and cogon grass [4]-[5] In nature, SiO_2 occurs in three forms: quartz, tridymite, and cristobalite, of which the transition temperatures (°C) and specific gravities are given in Table 1. SiO_2 melts at 1710°C and forms a transparent cooling glass. Chemically, it is relatively inert but is attacked by alkali or by hydrofluoric acid according to the equations:

$SiO_{2(s)} + 2NaOH_{(aq)} \rightarrow Na_2SiO_{3(aq)} + H_2O_{(l)}$

$SiO_{2(s)} + 4HF_{(aq)} \rightarrow SiF_{4(s)} + 2H_2O_{(l)}$

Table 1. Temperatures and specific gravities of SiO_2 form [6]

SiO_2 form	Temperature (°C)	Specific Gravity
Quartz	870	2.65
Tridymite	1470	2.26
Cristobalite	1470	2.32

*Corresponding author e-mail: dayupwardani@mipa.upr.ac.id.; (Dyah Ayu Pramoda Wardani).
Receive Date: 27 December 2021, Revise Date: 09 April 2022, Accept Date: 20 November 2022
DOI: 10.21608/EJCHEM.2022.107057.5148

The crystals of all three forms consist of three-dimensional SiO_2 tetrahedral networks joined. Each oxygen atom is typical to two tetrahedral fragments and situated midway between the silicon atoms [6]. Thus, the empirical formula for such a substance would be $(SiO_2)n$. The tetrahedral fragments form a spiral and are optically active (i.e., change the plane of polarization of incident light) [7] .

It is generally well-known that SiO_2 has unique physicochemical properties such as high hardness, water resistance, thermal resistance, and stiffness [8]. Silicon dioxide is widely used for various purposes with various sizes depending on the application needed, such as in the tire industry [9], rubber [10], glass [11], cement, concrete, ceramics [12], textiles [13], paper [14], cosmetics [15], electronics, paints [16], films [17], toothpaste, adsorbents, cordierite, and aluminosilicates [18]–[20], including high-reflection coatings, anti-reflection coatings, all-dielectric mirrors, beam dividers, bandpass filters, and polarizers [21].

The high degree of inconsistency between various SiO_2 surface studies has been attributed to the different preparation methods [22]. Many studies have been performed on dried gels or powders obtained by fuming [23] or sol-gel extraction [24]–[25] and processed by a variety of chemical, mechanical, thermal procedures [22]–[26], and annealing by means of laser beams [27].

Annealing is a heat treatment process that changes the physical and sometimes also the chemical properties of a material to increase ductility and reduce the hardness to make it more workable. Silicon dioxide annealing uses a high-temperature furnace to relieves stress in silicon. The heat activates ion-implanted dopants, reduces structural defects and stress, and reduces interface charge at the silicon-silicon dioxide interface [28].

Annealing processes has been reported possible to obtain crystalline or amorphous aggregates with different sizes and distributions embedded into a SiO_x matrix [29], at elevated temperatures (T ~> 1000 °C) may result in epitaxial alignment of polycrystalline silicon [27], to decrease or even eliminate thermal stress of SiO_2 glass so improve the stability of glass structure and properties [30] and in inert ambient is promising to improve the SiO_2/Si interface [31].

In this study, the FTIR, spectrometry UV-Vis diffuse reflectance, and SEM techniques were used to investigate the transformation of functional groups, band gap energy, and morphological properties of silicon dioxide (SiO_2) at various annealed temperatures.

2. Experimental

The material in this study was SiO_2 powder (Sigma-Aldrich 99%, USA). The equipment used in this study were furnaces, analytical balances, and porcelain crucibles. The method used consist of annealing and characterization. Furthermore, the SiO_2 powder was annealed with temperature variations at 0 (no treatment, room temperature), 800 °C, 900 °C, and 1000 °C (denoted as S0, S800, S900, and S1000) for 1 hour with increasing temperature 1,67 °C/minutes or 100 °C/hour. After that, the samples were allowed to cool down and characterized using FTIR, UV-Vis, and SEM. And then, the functional groups of annealed SiO_2 were characterized using FTIR Shimadzu IR Prestige 21, UV Vis-DR Analytic Jena Specord 200 Plus 13 was used in range 200 to 100 nm to get the value of absorbance. It was calculated in the Tauc plot method to get the band gap energy values of annealed SiO_2. Morphology of annealed SiO_2 was characterized using SEM JEOL/EO JSM-6510 versi 1.0, with a magnification of 10000x.

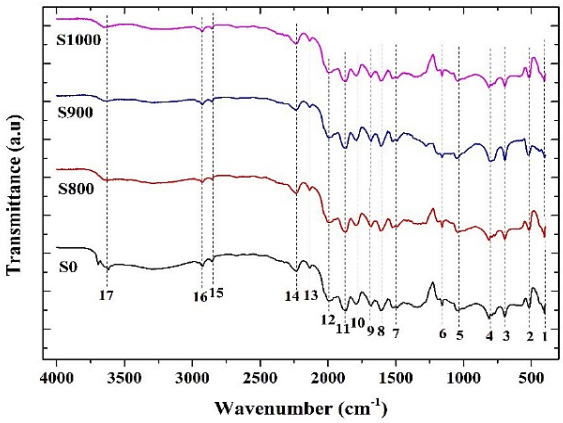

Figure 1. FTIR spectrum of annealed silicon dioxide (SiO_2)

3. Result and Discussion

3.1. Functional Groups Analysis of Annealed SiO_2

FTIR characterization was carried out by identifying the functional groups in a compound containing silicon dioxide (SiO_2), which had been annealed at S0, S800, S900, and S1000. The FTIR spectrums of annealed silicon dioxide (SiO_2) are shown in Fig. 1. The functional groups that appear are Si−O−Si, Si−Si, O−H, N=O, H−Si−Si−H (Monohidrida), and Si−OH, the wavenumber data (cm^{-1}) is presented in Table 2.

Table 2. Functional groups and wavenumber (cm^{-1}) of annealed SiO_2

No	Functional Group	Wavenumber (cm^{-1}) of annealed SiO_2			
		S0	S800	S900	S1000
1	Si−O−Si bending vibration	405	405	403	403
2	Si−O−Si bending vibration	517	518	520	516
3	Si−O symmetrical stretching vibration of Si−O−Si	696	696	694	696
4	Si–Si, Si−O stretching vibration	812	812	796	812
5	Si−O asymmetric stretching vibration	1041	1037	1051	1039
6	Si−O asymmetric stretching vibration	1159	1159	1159	1159
7	N=O	1517	1517	1519	1517
8	−OH bending vibration of Si−OH	1612	1604	1608	1602
9	−OH bending vibration of Si−OH	1681	1681	1681	1681
10	−OH bending vibration of Si−OH	1788	1788	1791	1789
11	−OH bending vibration of Si−OH	1867	1869	1869	1865
12	H−Si−Si−H (Monohidride)	1996	1998	1992	1992
13	H−Si−Si−H (Monohidride)	2133	2133	2137	2137
14	Si−O stretching vibration of Si−O−Si	2233	2233	2235	2239
15	−OH of Si−OH dan H_2O	2854	2854	2854	2854
16	−OH of Si−OH dan H_2O	2956	2976	2922	1226
17	−OH of Si−OH dan H_2O	3624	3631	3631	3644

Table 2 shows the appearance of the absorption band of the silanol group in the wavenumber region of 3700-2500 cm^{-1} (stretching vibration of −OH from Si−OH and H_2O) [32], the absorption band in the area of 1800-1600 cm^{-1} (bending vibration −OH from Si−OH) [33], and 1000-900 cm^{-1} (stretching vibration of Si−O from Si−OH) [33]. Siloxane groups are indicated by absorption bands in the wavenumber region of 2200-2500 cm^{-1} (bending vibration of Si−O from Si−O−Si) [34], 1100-1000 cm^{-1} (Si−O stretching vibration from Si−O−Si) [8], 850 – 650 cm^{-1} (Si−O symmetric stretching vibration from Si−O−Si) [35], and 500-400 cm^{-1} (bending vibration of Si−O−Si) [35]. Monohydride group with absorption band in region of 2150-1900 cm^{-1} (H−Si−Si−H vibration) [36].

Si-OH functional group decreases at wavenumber 3624-3644 cm^{-1}, and O–H at wavenumber 2922-2956 cm^{-1} indicates that with the increase of annealing temperature, the water content that interacts with SiO_2 decreases and oxidized to form Si−O−Si at 405-696 cm^{-1} and Si–Si at 796-812 cm^{-1}. Most of the isolated and germinal hydroxyl groups are thermally removed in 600-900 ºC. A series of annealing experiments in the temperature range from 100 to 870 ºC was studied to indicates the thermal stability of silanol. The hydrogen-bonded methanol coverage corresponds to the hydroxyl coverage was assumed in this experiment. After annealing, the Si−OH coverage was determined by exposing the surface to a saturation methanol exposure at 150 K (at a particular temperature) [37].

3.2. Band Gap Energy Analysis of Annealed SiO_2

One of the electrical properties of materials is band gap energy. The study of electrical properties, especially the determination of band gap energy, is determined through the material's absorption spectrum. The absorption spectrum of the material was obtained using a UV-Vis spectrophotometer [38].

Based on electrical conductivity, material properties are grouped into insulators, semiconductors, and conductors. The material's physical properties are generally determined by the magnitude of the electrical conductivity (σ_m) and the band gap energy (E_g) [39].

The band gap energy of annealed silicon dioxide at S0, S800, S900, and S1000 was determined by analyzing the absorbance values using UV-Vis DR with a wavenumber range of 200 to 1100 nm. Quantitatively, the band gap energy was calculated using the Tauc plot method with a direct transition (direct plot). The energy gap produced of SiO_2 annealed can determine by the UV-Vis Diffuse Reflectance spectrophotometric method. This method is based on measuring the UV-Vis intensity reflected by the sample.

The band gap energy is the difference between the upper end of the valence band (E_v) and the lower end of the conduction band (E_c) or the minimum energy required to excite electrons from the valence band to the conduction band [40].

The Tauc plot method determines the optical band gap by looking at a linear graph of the relationship E (eV) on the x-axis and $(ahv)^{1/m}$ y-axis. The relationship between photon energy (hv) and absorption coefficient (α) is determined by the equation:

$$(\alpha hv)^{1/m} = c(hv - Eg) \quad (1)$$

where h = $6{,}63 \times 10^{-34}\ J \cdot s$, c is the speed constant of light and E_g is the material energy gap and the exponent m depends on the type of transition [41].

Extrapolation of the linear portion of the plots of $(\alpha h\upsilon)^2$ versus photon energy to $\alpha = 0$ yields the optical band gap of annealed SiO_2, the direct transition plot of annealed silicon dioxide (SiO_2) [42] is presented in Fig. 2 and the band gap energy values are presented in Table 3. Table 3 shows that the band gap energy value of annealed SiO_2 decreases with increasing annealing temperature. This is related to eliminating the defect and decreasing the defect state in the energy gap.

Table 3. Energy Band Gap of Annealed SiO_2

Annealed SiO_2	Energy Band Gap (eV)
S0	2,27
S800	2,27
S900	2,26
S1000	2,22

3.3. Morphology of Silicon Dioxide (SiO_2)

The morphology of silicon dioxide (SiO_2) was analyzed using SEM. The powder SiO_2 samples had a characteristic high degree of weathering and flake-like impurities distributed between SiO_2 particles or on the surface of SiO_2 particles. A part of it was wrapped in weathered SiO_2 particles or mingled in SiO_2 particle gaps. The increase in annealing temperature also impacts the surface roughness of SiO_2. Fig. 3 shows the annealed silicon dioxide (SiO_2) at S0, S800, S900, and S1000. In the previous study, annealed silicon dioxide (SiO_2) XRD patterns show that the sample was quartz crystal [43]. Annealed SiO_2 has irregular shape and particle size, probably due to the annealing temperature treatment given. This morphology is consistent with the experiments which reported that the silicon dioxide particles were irregular geometry and jagged [44]–[45]. Each spot was about 3-10 µm in diameter and the given content of impurity elements thus determined as semi-quantitative.

The increase in the annealing temperature indicates a slight agglomeration and larger particle size. Then the roughness level becomes smaller thereby decreasing its hydrophobicity. The particle size increases with increasing annealing temperature caused by the greater the thermal energy received in structure of silicon dioxide (SiO_2) [46].

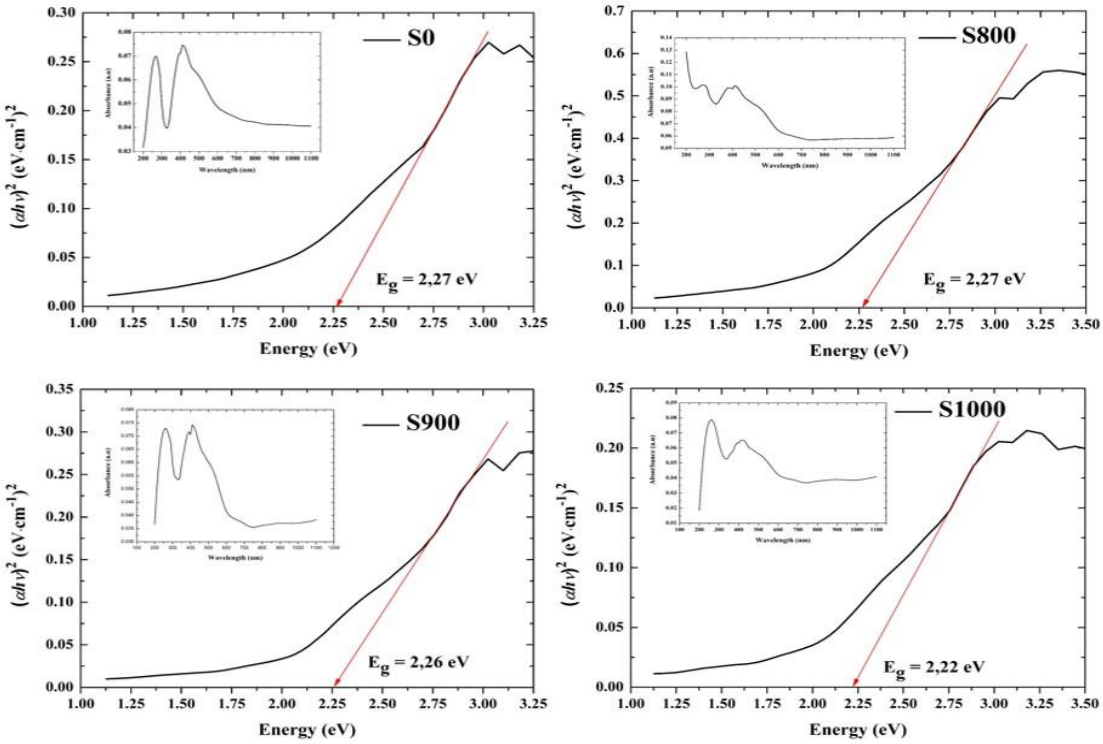

Figure 2. The Tauc plot of annealed SiO_2

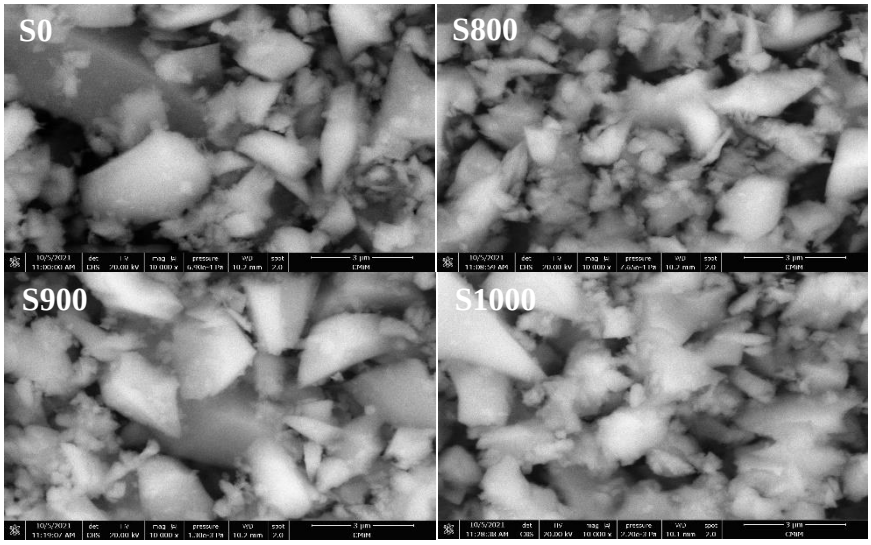

Figure 3. Morphology of annealed silicon dioxide (SiO_2)

4. Conclusions

The qualitative analysis confirmed that annealed SiO_2 had characterized functional groups of annealed silicon dioxide: Si−O−Si, Si−Si, −OH, H−Si−Si−H (monohydride), and Si−OH. The band gap energy values for annealed SiO_2 at 0 (without treatment), 800 °C, 900 °C and 1000 °C were 2.27; 2.27; 2.26; 2.22 eV. The morphology of silicon dioxide shows that silicon dioxide has an irregular shape and size. It has acute angles accompanied by small flakes on the surface, and the particle size is estimated to be around 3-10 μm.

5. Acknowledgments

This research was funded by PKPT Grant (No. 264/UN24.13/PL/2021) by the Ministry of Education and Culture, Research and Technology of the Republic of Indonesia (Kementerian Pendidikan dan Kebudayaan, Riset, dan Teknologi Republik Indonesia).

6. References

[1] H. Füchtbauer, “Sedimente und sedimentgesteine,” 2009.

[2] K. H. Wedepohl, C. W. Correns, D. M. Shaw, K. K. Turekian, and J. Zemann, “Handbook of geochemistry,” 1969.

[3] R. D. Aines, S. H. Kirby, and G. R. Rossman, “Hydrogen speciation in synthetic quartz,” *Phys. Chem. Miner.*, vol. 11, no. 5, pp. 204–212, 1984, doi: https://doi.org/10.1007/BF00308135.

[4] I. Irzaman, D. Yustaeni, A. Aminullah, I. Irmansyah, and B. Yuliarto, “Purity, Morphological, and Electrical Characterization of Silicon Dioxide from Cogon Grass (Imperata cylindrica) Using Different Ashing Temperatures,” *Egypt. J. Chem.*, vol. 64, no. 8, pp. 4143–4149, 2021, DOI: 10.21608/EJCHEM.2019.15430.1962.

[5] I. Irzaman, I. D. Cahyani, A. Aminullah, A. Maddu, B. Yuliarto, and U. Siregar, “Biosilica properties from rice husk using various HCl concentrations and frequency sources,” *Egypt. J. Chem.*, vol. 63, no. 2, pp. 363–371, 2020, doi: DOI: 10.21608/ejchem.2019.8044.1679.

[6] G. Raj, *Advanced Inorganic Chemistry Vol-1*. Krishna Prakashan Media, 2008.

[7] X. Shi, N. S. Dalai, X. N. Hu, and V. Vallyathan, “The chemical properties of silica particle surface in relation to silica-cell interactions,” *J. Toxicol. Environ. Heal. Part A Curr. Issues*, vol. 27, no. 4, pp. 435–454, 1989, doi: https://doi.org/10.1080/15287398909531314.

[8] F. Adam, K. Kandasamy, and S. Balakrishnan, “Iron incorporated heterogeneous catalyst from rice husk ash,” *J. Colloid Interface Sci.*, vol. 304, no. 1, pp. 137–143, 2006, doi: https://doi.org/10.1016/j.jcis.2006.08.051.

[9] N. H. N. A. Hadi, A. Anuar, and R. K. Shuib, “Effect of Different Salinization Methods of Silica Filler on Rubber Reinforcement,” *J. Eng.*, vol. 15, no. 2, pp. 71–81, 2019, doi: https://doi.org/10.21315/jes2019.15.2.5.

[10] S. Begum, M. Allaudin, M. A. Qaiser, and F. Khan, “Beneficiation of silica sand for the manufacturing of optical glass,” *Journal-Chemical Soc. Pakistan*, vol. 21, no. 2, pp. 83–86, 1999.

[11] N. K. Amudhavalli and J. Mathew, “Effect of silica fume on strength and durability parameters of concrete,” *Int. J. Eng. Sci. \& Emerg. Technol.*, vol. 3, no. 1, pp. 28–35, 2012, doi: ISSN: 2231 – 6604.

[12] M. Sahri, A. R. Tualeka, and N. Widajati, “Quantitative risk assesment of crystalline silica exposure in ceramics industry,” *Indian J. Public Heal. Res. \& Dev.*, vol. 10, no. 2, pp. 601–604, 2019, [Online]. Available: http://repository.unusa.ac.id/id/eprint/5841.

[13] A. Berendjchi, R. Khajavi, and M. E. Yazdanshenas, “Application of nanosols in textile industry,” *Int. J. Green Nanotechnol.*, vol. 1, p. 1943089213506814, 2013, doi: https://doi.org/10.1177%2F1943089213506814.

[14] A. F. Lourenço, J. A. F. Gamelas, J. Sequeira, P. J. Ferreira, and J. L. Velho, “Improving paper mechanical properties using silica-modified ground calcium carbonate as filler,”

BioResources, vol. 10, no. 4, pp. 8312–8324, 2015, [Online]. Available: http://hdl.handle.net/10316/30029.

[15] S. Nafisi and M. Maibach, "Silica nanoparticles for increased cosmetic ingredient efficacy," *Cosmet. Toilet*, vol. 130, pp. 36–43, 2015.

[16] C.-M. Lehr, "Case Study: Paints and Lacquers with Silica Nanoparticles," in *Safety of Nanomaterials along Their Lifecycle*, CRC Press, 2014, pp. 410–427.

[17] P. Y. Steinberg *et al.*, "Structural and mechanical properties of silica mesoporous films synthesized using deep X-rays: implications in the construction of devices," *Front. Mater.*, vol. 8, p. 27, 2021, doi: https://doi.org/10.3389/fmats.2021.628245.

[18] S. Sembiring, W. Simanjuntak, R. Situmeang, A. Riyanto, and K. Sebayang, "Preparation of refractory cordierite using amorphous rice husk silica for thermal insulation purposes," *Ceram. Int.*, vol. 42, no. 7, pp. 8431–8437, 2016,doi: https://doi.org/10.1016/j.ceramint.2016.02.062.

[19] W. Simanjuntak, S. Sembiring, P. Manurung, R. Situmeang, and I. M. Low, "Characteristics of aluminosilicates prepared from rice husk silica and aluminum metal," *Ceram. Int.*, vol. 39, no. 8, pp. 9369–9375, 2013, doi: https://doi.org/10.1016/j.ceramint.2013.04.112.

[20] L. Sun and K. Gong, "Silicon-based materials from rice husks and their applications," *Ind. \& Eng. Chem. Res.*, vol. 40, no. 25, pp. 5861–5877, 2001, doi: https://doi.org/10.1021/ie010284b.

[21] I. S. Naji, N. A. Khalifa, and H. M. Khalaf, "Influence of annealing temperature on the physical properties of thin Cu_2SiO_4 films prepared by pulsed laser deposition," *Dig. J. Nanomater. BIOSTRUCTURES*, vol. 12, no. 3, pp. 899–907, 2017.

[22] R. K. Iler, *The colloid chemistry of silica and silicates*, vol. 80, no. 1. LWW, 1955.

[23] C. P. Tripp and M. L. Hair, "Measurement of polymer adsorption on colloidal silica by in situ transmission Fourier transform infrared spectroscopy," *Langmuir*, vol. 9, no. 12, pp. 3523–3529, 1993, doi: https://doi.org/10.1021/la00036a030.

[24] D. W. Sindorf and G. E. Maciel, "Silicon-29 NMR study of dehydrated/rehydrated silica gel using cross polarization and magic-angle spinning," *J. Am. Chem. Soc.*, vol. 105, no. 6, pp. 1487–1493, 1983, doi: https://doi.org/10.1021/ja00344a012.

[25] R. Guermeur, C. Jacolin, F. Biquard, and C. Blanc, "Microwave dielectric measurements on nitrogen adsorbed on silica: Isothermal kinetics of adsorption," *Surf. Sci.*, vol. 255, no. 1–2, pp. 157–175, 1991, doi: https://doi.org/10.1016/0039-6028(91)90018-N.

[26] D. Mazouzi *et al.*, "New insights into the silicon-based electrode's irreversibility along cycle life through simple gravimetric method," *J. Power Sources*, vol. 220, pp. 180–184, 2012, doi: https://doi.org/10.1016/j.jpowsour.2012.08.007.

[27] V. G. Lifshits, I. G. Kaverina, V. V Korobtsov, A. A. Saranin, and A. V Zotov, "Thermal annealing behaviour of Si/SiO_2 structures," *Thin Solid Films*, vol. 135, no. 1, pp. 99–105, 1986, doi: https://doi.org/10.1016/0040-6090(86)90092-1.

[28] F. Ravaux, N. S. Rajput, J. Abed, L. George, M. Tiner, and M. Jouiad, "Effect of rapid thermal annealing on crystallization and stress relaxation of SiGe nanoparticles deposited by ICP PECVD," *RSC Adv.*, vol. 7, no. 51, pp. 32087–32092, 2017, doi: DOI: 10.1039/C7RA04426G.

[29] K. Kayed and D. B. Kurd, "The effect of annealing temperature on the structural and optical properties of Si/SiO_2 composites synthesized by thermal oxidation of silicon wafers," *Silicon*, pp. 1–7, 2021, doi: https://doi.org/10.1007/s12633-021-01307-w.

[30] Y. Su, H. Yin, X. He, and Y. Zhou, "Influence of annealing on the structure of silica glass," *J. Wuhan Univ. Technol. Sci. Ed.*, vol. 28, no. 5, pp. 902–906, 2013, doi: https://doi.org/10.1007/s11595-013-0790-6.

[31] N. Balaji, C. Park, S. Chung, M. Ju, J. Raja, and J. Yi, "Effects of low temperature anneal on the interface properties of thermal silicon oxide for silicon surface passivation," *J. Nanosci. Nanotechnol.*, vol. 16, no. 5, pp. 4783–4787, 2016, doi: https://doi.org/10.1166/jnn.2016.12178.

[32] U. Kalapathy, A. Proctor, and J. Shultz, "Silica xerogels from rice hull ash: structure, density and mechanical strength as affected by gelation pH and silica concentration," *J. Chem. Technol. \& Biotechnol.*, vol. 75, no. 6, pp. 464–468, 2000, doi: https://doi.org/10.1002/1097-4660(200006)75:6%3C464::AID-JCTB235%3E3.0.CO;2-C.

[33] K. C. Wong, "Review of spectrometric identification of organic compounds." ACS Publications, 2015, doi: https://doi.org/10.1021/acs.jchemed.5b00571.

[34] M. D. Astuti, R. Nurmasari, and D. R. Mujiyanti, "Imobilisasi 1, 8-dihidroxyanthraquinon pada silika gel melalui proses sol-gel," 2012, [Online]. Available: https://repo-dosen.ulm.ac.id//handle/123456789/20744.

[35] E. W. Juni, A. Arnelli, and S. Sriatun, "Pemanfaatan Surfaktan Kationik Hasil Sublasi sebagai Molekul Pengarah pada Pembuatan Material Berpori dari Sekam Padi," *J. Kim. Sains dan Apl.*, vol. 15, no. 1, pp. 24–28, 2012, doi: https://doi.org/10.14710/jksa.15.1.24-28.

[36] L. H. Abuhassan, "Enhancement of the production yield of fluorescent silicon nanostructures using silicon-based salts," *Sains Malaysiana*, vol. 39, no. 5, pp. 837–844, 2010.

[37] O. Sneh and S. M. George, "Thermal stability of hydroxyl groups on a well-defined silica surface," *J. Phys. Chem.*, vol. 99, no. 13, pp. 4639–4647, 1995, doi: https://doi.org/10.1021/j100013a039.

[38] Z. S. Ngara, "Metode Fisika Eksperimen (Pengukuran Dan Analisis Data Eksperimen Fisika)," *Kupang, Penerbit Gita Kasih*, 2014.

[39] W. D. Callister Jr and D. G. Rethwisch, *Fundamentals of materials science and engineering: an integrated approach*.

John Wiley \& Sons, 2020.

[40] S. M. Sze, *Semiconductor devices: physics and technology*. John wiley \& sons, 2008.

[41] R. Sarkar, C. S. Tiwary, P. Kumbhakar, S. Basu, and A. K. Mitra, "Yellow-orange light emission from Mn^{2+}-doped ZnS nanoparticles," *Phys. E Low-dimensional Syst. Nanostructures*, vol. 40, no. 10, pp. 3115–3120, 2008, doi: https://doi.org/10.1016/j.physe.2008.04.013.

[42] I. S. Naji, "Study the effect of thermal annealing on some physical properties of thin Cu_2SiO_3 films prepared by pulsed laser deposition," *Iraqi J. Phys.*, vol. 15, no. 35, pp. 148–157, 2018, doi: 10.30723/ijp.v15i35.64.

[43] B. Hariyanto, D. A. P. Wardani, N. Kurniawati, N. P. Har, N. Darmawan, and others, "X-Ray Peak Profile Analysis of Silica by Williamson--Hall and Size-Strain Plot Methods," in *Journal of Physics: Conference Series*, 2021, vol. 2019, no. 1, p. 12106, doi: https://doi.org/10.1088/1742-6596/2019/1/012106.

[44] M. A. Azmi, N. A. A. Ismail, M. Rizamarhaiza, and H. Taib, "Characterisation of silica derived from rice husk (Muar, Johor, Malaysia) decomposition at different temperatures," in *AIP Conference Proceedings*, 2016, vol. 1756, no. 1, p. 20005, doi: https://doi.org/10.1063/1.4958748.

[45] I. J. Fernandes *et al.*, "Characterization of silica produced from rice husk ash: comparison of purification and processing methods," *Mater. Res.*, vol. 20, pp. 512–518, 2017, doi: https://doi.org/10.1590/1980-5373-MR-2016-1043.

[46] F. Milah, "Pengaruh Variasi Temperatur Annealing terhadap Sifat Hidrofobik Lapisan SiO_2 pada Kaca," Institut Teknologi Sepuluh Nopember, 2018.